



Stability of discrete solitons in nonlinear Schrödinger lattices

D.E. Pelinovsky^a, P.G. Kevrekidis^{b,*}, D.J. Frantzeskakis^c

^a Department of Mathematics, McMaster University, Hamilton, Ontario, Canada L8S 4K1

^b Department of Mathematics, University of Massachusetts, Amherst, MA, 01003-4515, USA

^c Department of Physics, University of Athens, Panepistimiopolis, Zografos, Athens 15784, Greece

Received 11 August 2004; received in revised form 24 January 2005; accepted 11 July 2005

Available online 2 November 2005

Communicated by C.K.R.T. Jones

Abstract

We consider the discrete solitons bifurcating from the anti-continuum limit of the discrete nonlinear Schrödinger (NLS) lattice. The discrete soliton in the anti-continuum limit represents an arbitrary finite superposition of *in-phase* or *anti-phase* excited nodes, separated by an arbitrary sequence of empty nodes. By using stability analysis, we prove that the discrete solitons are all unstable near the anti-continuum limit, except for the solitons, which consist of alternating anti-phase excited nodes. We classify analytically and confirm numerically the number of unstable eigenvalues associated with each family of the discrete solitons.

© 2005 Elsevier B.V. All rights reserved.

Keywords: Discrete nonlinear Schrödinger equation; Discrete solitons; Existence and stability; Lyapunov–Schmidt reductions

1. Introduction

Nonlinear instabilities and the emergence of coherent structures in differential–difference equations have become topics of physical importance and mathematical interest in the past decade. Numerous applications of these problems have emerged ranging from nonlinear optics, in the dynamics of guided waves in inhomogeneous optical structures [1,2] and photonic crystal lattices [3,4], to atomic physics, in the dynamics of Bose–Einstein condensate droplets in periodic (optical lattice) potentials [5–8] and from condensed matter, in Josephson-junction ladders [9,10], to biophysics, in various models of the DNA double strand [11,12]. This large range of models and applications has been summarized in a variety of reviews such as [13–17].

* Corresponding author.

E-mail address: kevrekid@math.umass.edu (P.G. Kevrekidis).

One of the prototypical differential–difference models that is both physically relevant and mathematically tractable is the so-called discrete nonlinear Schrödinger (NLS) equation,

$$i\dot{u}_n + \varepsilon \Delta_d u_n + \gamma |u_n|^2 u_n = 0, \quad (1.1)$$

where $u_n = u_n(t)$ is a complex amplitude in time t , $n \in \mathbb{Z}^d$ is the d -dimensional lattice, Δ_d is the d -dimensional discrete Laplacian (the “standard” one constructed out of three-point stencils in each lattice direction), ε is the dispersion coefficient, and γ is the nonlinearity coefficient. Before we delve into mathematical analysis of the discrete NLS equation, it is relevant to discuss briefly the recent physical applications of this model.

The most direct implementation of the discrete NLS-type equations can be identified in one-dimensional arrays of coupled optical waveguides [1,2]. These may be multi-core structures created in a slab of a semiconductor material (such as AlGaAs), or virtual ones, induced by a set of laser beams illuminating a photorefractive crystal. In this experimental implementation, there are about forty lattice sites (guiding cores), and the localized modes (discrete solitons) may propagate over many diffraction lengths.

Light-induced photonic lattices [3,4] have recently emerged as an important application of such equations. The refractive index of the nonlinear photonic lattices changes periodically due to a grid of strong beams, while a weaker probe beam is used to monitor the localized modes (discrete solitons). A number of promising experimental studies of discrete solitons in light-induced photonic lattices were reported recently in the physics literature.

An array of Bose–Einstein condensate droplets trapped in a strong optical lattice with thousands of atoms in each droplet is another direct physical realization of the discrete NLS equation [5,6]. In this context, the model can be derived systematically by using the Wannier function expansions [7,8].

Besides applications to optical waveguides, photonic crystal lattices, and Bose–Einstein condensates trapped in optical lattices, the discrete NLS equation also arises as the envelope wave reduction of the general nonlinear Klein–Gordon lattices [18].

This rich variety of physical contexts makes it timely and relevant to analyze the mathematical aspects of the discrete NLS equation (1.1), including the existence and stability of localized modes (discrete solitons). A very helpful tool for such an analysis is the so-called anti-continuum limit $\varepsilon \rightarrow 0$ [13], where the nonlinear oscillators of the model are uncoupled. The existence of localized modes in this limit can be characterized in full detail [15]. The persistence, multiplicity, and stability of localized modes can be studied with continuation methods both analytically and numerically [19].

Our aim is to study localized modes of the discrete NLS equation (1.1) in two papers. The present paper describes the stability analysis of discrete solitons in the one-dimensional NLS lattice ($d = 1$). A separate work will present Lyapunov–Schmidt reductions for the persistence, multiplicity and stability of discrete vortices in the two-dimensional NLS lattice ($d = 2$).

This paper is structured as follows. We review the known results on the existence of one-dimensional discrete solitons in Section 2. General stability and instability results for discrete solitons in the anti-continuum limit are proved in Section 3. These stability results are illustrated for two particular families of the discrete solitons in Sections 4 and 5. Besides explicit perturbation series expansion results, we compare asymptotic approximations and numerical computations of stable and unstable eigenvalues in the linearized stability problem. Section 6 contains our conclusions.

2. Existence of discrete solitons

We consider the normalized form of the discrete NLS equation (1.1) in one dimension ($d = 1$):

$$i\dot{u}_n + \varepsilon(u_{n+1} - 2u_n + u_{n-1}) + |u_n|^2 u_n = 0, \quad (2.1)$$

where $u_n(t) : \mathbb{R}_+ \rightarrow \mathbb{C}$, $n \in \mathbb{Z}$, and $\varepsilon > 0$ is the inverse squared step size of the discrete one-dimensional NLS lattice. The discrete solitons are given by the time-periodic solutions of the discrete NLS equation (2.1):

$$u_n(t) = \phi_n e^{i(\mu-2\varepsilon)t + i\theta_0}, \quad \mu \in \mathbb{R}, \phi_n \in \mathbb{C}, n \in \mathbb{Z}, \quad (2.2)$$

where $\theta_0 \in \mathbb{R}$ is a parameter and (μ, ϕ_n) solve the nonlinear difference equations on $n \in \mathbb{Z}$:

$$(\mu - |\phi_n|^2)\phi_n = \varepsilon(\phi_{n+1} + \phi_{n-1}). \quad (2.3)$$

The existence of the discrete solitons was studied recently in [20–22], inspired by the pioneer papers [23,24]. A recent summary of the existence results is given in [19]. Since discrete solitons in the focusing NLS lattice (2.1) only exist for $\mu > 2\varepsilon$ [19] and the parameter μ is scaled out by the scaling transformation

$$\phi_n = \sqrt{\mu} \hat{\phi}_n, \quad \varepsilon = \mu \hat{\varepsilon}, \quad (2.4)$$

the parameter μ will henceforth be set as $\mu = 1$. Another arbitrary parameter θ_0 , which exists due to the gauge invariance of the discrete NLS equation (2.1), is incorporated in the ansatz (2.2) such that at least one value of ϕ_n can be chosen real valued without lack of generality. Using this convention, we represent below the known existence results.

Proposition 2.1. *There exist $\varepsilon_0 > 0$, $\kappa > 0$ and $\phi_\infty > 0$ such that the difference equations (2.3) with $\mu = 1$ and $0 < \varepsilon < \varepsilon_0$ have continuous families of discrete solitons with the properties:*

(i)

$$\lim_{\varepsilon \rightarrow 0^+} \phi_n = \phi_n^{(0)} = \begin{cases} e^{i\theta_n}, & n \in S, \\ 0, & n \in \mathbb{Z} \setminus S, \end{cases} \quad (2.5)$$

(ii)

$$\lim_{|n| \rightarrow \infty} e^{\kappa|n|} |\phi_n| = \phi_\infty, \quad (2.6)$$

(iii)

$$\phi_n \in \mathbb{R}, \quad n \in \mathbb{Z}, \quad (2.7)$$

where S is a finite set of nodes of the lattice $n \in \mathbb{Z}$ and $\theta_n = \{0, \pi\}$, $n \in S$.

Proof. See Theorem 2.1 and Appendices A and B in [19] for the proof of the limiting solution (2.5) from the inverse function theorem. See Theorem 3 in [24] for the proof of the exponential decay (2.6) from the bound estimates. See Section 3.2 in [15] for the proof of the reality condition (2.7) from the conservation of the density current. Various theoretical and numerical bounds on ε_0 are obtained in [15,19,20,24]. \square

Due to the property (2.7), the difference equations (2.3) with $\mu = 1$ can be rewritten as follows:

$$(1 - \phi_n^2)\phi_n = \varepsilon(\phi_{n+1} + \phi_{n-1}), \quad n \in \mathbb{Z}. \quad (2.8)$$

For our analysis, we shall derive two technical results on properties of solutions ϕ_n , $n \in \mathbb{Z}$.

Lemma 2.2. *There exists $\varepsilon_0 > 0$ such that the solution ϕ_n , $n \in \mathbb{Z}$, is represented by the convergent power series for $0 \leq \varepsilon < \varepsilon_0$:*

$$\phi_n = \phi_n^{(0)} + \sum_{k=1}^{\infty} \varepsilon^k \phi_n^{(k)}, \quad (2.9)$$

where $\phi_n^{(0)}$ is given by (2.5).

Proof. The statement follows from the Implicit Function Theorem (see Theorem 2.7.2 in [25]), since the Jacobian matrix for the system (2.8) is non-singular at $\phi_n = \phi_n^{(0)}$, $n \in \mathbb{Z}$, while the right-hand side of the system (2.8) is analytic in ε . \square

Lemma 2.3. *There exists $0 < \varepsilon_1 < \varepsilon_0$ such that the number of changes in the sign of ϕ_n on $n \in \mathbb{Z}$ for $0 < \varepsilon < \varepsilon_1$ is equal to the number of π -differences of the adjacent θ_n , $n \in S$, in the limiting solution (2.5).*

Proof. Consider two adjacent excited nodes $n_1, n_2 \in S$ separated by N empty nodes such that $n_2 - n_1 = 1 + N$ and $N \geq 1$. We need to prove that the number of π -differences in the argument of ϕ_n , $n_1 \leq n \leq n_2$, for small $\varepsilon > 0$ is exactly one if $\theta_{n_2} - \theta_{n_1} = \pi$ and zero if $\theta_{n_2} - \theta_{n_1} = 0$. To do so, we consider the difference equations (2.8) on $n_1 < n < n_2$ as the N -by- N matrix system

$$\mathcal{A}_N \boldsymbol{\phi}_N = \varepsilon \mathbf{b}_N, \quad (2.10)$$

where $\boldsymbol{\phi}_N = (\phi_{n_1+1}, \dots, \phi_{n_2-1})^T$, and

$$\mathcal{A}_N = \begin{pmatrix} 1 - \phi_{n_1+1}^2 & -\varepsilon & 0 & \cdots & 0 \\ -\varepsilon & 1 - \phi_{n_1+2}^2 & -\varepsilon & \cdots & 0 \\ \vdots & \vdots & \vdots & \cdots & \vdots \\ 0 & 0 & 0 & \cdots & 1 - \phi_{n_2-1}^2 \end{pmatrix}, \quad \mathbf{b}_N = \begin{pmatrix} \phi_{n_1} \\ 0 \\ \vdots \\ \phi_{n_2} \end{pmatrix}. \quad (2.11)$$

Let $D_{I,J}$, $1 \leq I \leq J \leq N$, be the determinant of the block of the matrix \mathcal{A}_N between the I -th and J -th rows and columns. By Cramer's rule, we have

$$\phi_{n_1+j} = \frac{\varepsilon^j \phi_{n_1} D_{j+1,N} + \varepsilon^{N-j+1} \phi_{n_2} D_{1,N-j}}{D_{1,N}}. \quad (2.12)$$

Since $\lim_{\varepsilon \rightarrow 0} D_{I,J} = 1$ for all $1 \leq I \leq J \leq N$, we have

$$\begin{aligned} \lim_{\varepsilon \rightarrow 0} \varepsilon^{-j} \phi_{n_1+j} &= \phi_{n_1}, & 1 \leq j < \frac{N+1}{2}, \\ \lim_{\varepsilon \rightarrow 0} \varepsilon^{-j} \phi_{n_1+j} &= \phi_{n_1} + \phi_{n_2}, & j = \frac{N+1}{2}, \\ \lim_{\varepsilon \rightarrow 0} \varepsilon^{j-1-N} \phi_{n_1+j} &= \phi_{n_2}, & \frac{N+1}{2} < j \leq N. \end{aligned}$$

The statement of Lemma follows from the signs of ϕ_n , $n_1 \leq n \leq n_2$, for small $\varepsilon > 0$. \square

By Proposition 2.1 and Lemma 2.3, all families of the discrete solitons as $\varepsilon \rightarrow 0$ can be classified by a sequence of $\{0\}$, $\{+\}$, and $\{-\}$ of the limiting solution (2.5) on the finite set S [19]. In particular, we consider two ordered sets S :

$$S_1 = \{1, 2, 3, \dots, N\} \quad (2.13)$$

and

$$S_2 = \{1, 3, 5, \dots, 2N - 1\}, \quad (2.14)$$

where $\dim(S_1) = \dim(S_2) = N < \infty$. The set S_1 includes the Page mode ($N = 2$: $\theta_1 = \theta_2 = 0$) and the twisted mode ($N = 2$: $\theta_1 = 0, \theta_2 = \pi$). The set S_2 includes the Page and twisted modes ($N = 2$), separated by an empty node.

3. Stability of discrete solitons

The spectral stability of discrete solitons is studied with the standard linearization

$$u_n(t) = e^{i(1-2\varepsilon)t + i\theta_0} (\phi_n + a_n e^{\lambda t} + \bar{b}_n e^{\bar{\lambda} t}), \quad \lambda \in \mathbb{C}, (a_n, b_n) \in \mathbb{C}^2, n \in \mathbb{Z}, \quad (3.1)$$

where (λ, a_n, b_n) solve the linear eigenvalue problem on $n \in \mathbb{Z}$:

$$\begin{aligned} (1 - 2\phi_n^2)a_n - \phi_n^2 b_n - \varepsilon(a_{n+1} + a_{n-1}) &= i\lambda a_n, \\ -\phi_n^2 a_n + (1 - 2\phi_n^2)b_n - \varepsilon(b_{n+1} + b_{n-1}) &= -i\lambda b_n. \end{aligned} \tag{3.2}$$

The discrete soliton (2.2) is called spectrally unstable if there exist λ and (a_n, b_n) , $n \in \mathbb{Z}$, in the problem (3.2) such that $\text{Re}(\lambda) > 0$ and $\sum_{n \in \mathbb{Z}} (|a_n|^2 + |b_n|^2) < \infty$. Otherwise, the soliton is called weakly spectrally stable. Orbital stability of the discrete one-pulse soliton was studied in the anti-continuum limit $\varepsilon \rightarrow 0$ [26] and close to the continuum limit $\varepsilon \rightarrow \infty$ [27]. Spectral instabilities of two-pulse and multi-pulse solitons were considered in [28–33] using numerical and variational approximations. It was well understood from intuition supported by numerical simulations [13,32] that the discrete solitons with the alternating sequence of $\theta_n = \{0, \pi\}$ in the limiting solution (2.5) are spectrally stable as $\varepsilon \rightarrow 0$ but have eigenvalues with so-called negative Krein signature, which become complex by means of the Hamiltonian–Hopf bifurcations [29,33]. All other families of discrete solitons have unstable real eigenvalues λ in the anti-continuum limit for any $\varepsilon \neq 0$ [32].

Here we prove these preliminary observations and find the precise number of stable and unstable eigenvalues in the linearized stability problem (3.2) for small $\varepsilon > 0$. Our results are similar to those in the Lyapunov–Schmidt reductions, which are applied to continuous multi-pulse solitons in nonlinear Schrödinger equations [34–37]. In particular, the main conclusion on stability of alternating up–down solitons and instability of any other up–up and down–down sequences of solitons was found for multi-pulse homoclinic orbits arising in the so-called orbit-flip bifurcation [34, p. 176]. The same conclusion agrees with qualitative predictions for the discrete NLS equations [32, p. 66].

Let $\Omega = l^2(\mathbb{Z}, \mathbb{C})$ be the Hilbert space of square-summable bi-infinite complex-valued sequences $\{u_n\}_{n \in \mathbb{Z}}$, equipped with the inner product and norm

$$(\mathbf{u}, \mathbf{w})_\Omega = \sum_{n \in \mathbb{Z}} \bar{u}_n w_n, \quad \|\mathbf{u}\|_\Omega^2 = \sum_{n \in \mathbb{Z}} |u_n|^2 < \infty. \tag{3.3}$$

We use bold notation \mathbf{u} for an infinite-dimensional vector in Ω that consists of components u_n for all $n \in \mathbb{Z}$. The stability problem (3.2) is transformed with the substitution

$$a_n = u_n + iw_n, \quad b_n = u_n - iw_n, \quad n \in \mathbb{Z}, \tag{3.4}$$

to the form

$$\begin{aligned} (1 - 3\phi_n^2)u_n - \varepsilon(u_{n+1} + u_{n-1}) &= -\lambda w_n, \\ (1 - \phi_n^2)w_n - \varepsilon(w_{n+1} + w_{n-1}) &= \lambda u_n. \end{aligned} \tag{3.5}$$

The matrix–vector form of the problem (3.5) is

$$\mathcal{L}_+ \mathbf{u} = -\lambda \mathbf{w}, \quad \mathcal{L}_- \mathbf{w} = \lambda \mathbf{u}, \tag{3.6}$$

where \mathcal{L}_\pm are infinite-dimensional symmetric tri-diagonal matrices, which consist of the elements

$$(\mathcal{L}_+)_{n,n} = 1 - 3\phi_n^2, \quad (\mathcal{L}_-)_{n,n} = 1 - \phi_n^2, \quad (\mathcal{L}_\pm)_{n,n+1} = (\mathcal{L}_\pm)_{n+1,n} = -\varepsilon.$$

Equivalently, the stability problem (3.6) is rewritten in the Hamiltonian form

$$\mathcal{J}\mathcal{H}\psi = \lambda \psi, \tag{3.7}$$

where ψ is the infinite-dimensional eigenvector, which consists of 2-blocks of $(u_n, w_n)^T$, \mathcal{J} is the infinite-dimensional skew-symmetric matrix, which consists of 2-by-2 blocks of

$$\mathcal{J}_{n,m} = \begin{pmatrix} 0 & 1 \\ -1 & 0 \end{pmatrix} \delta_{n,m},$$

and \mathcal{H} is the infinite-dimensional symmetric matrix, which consists of 2-by-2 blocks of

$$\mathcal{H}_{n,m} = \begin{pmatrix} (\mathcal{L}_+)_{n,m} & 0 \\ 0 & (\mathcal{L}_-)_{n,m} \end{pmatrix}.$$

The representation (3.7) follows from the Hamiltonian structure of the discrete NLS equation (2.1), where \mathcal{J} is the symplectic operator and \mathcal{H} is the linearized Hamiltonian. By Lemma 2.2, the matrix \mathcal{H} is expanded into the power series

$$\mathcal{H} = \mathcal{H}^{(0)} + \sum_{k=1}^{\infty} \varepsilon^k \mathcal{H}^{(k)}, \quad (3.8)$$

where $\mathcal{H}^{(0)}$ is diagonal with two blocks:

$$\mathcal{H}_{n,n}^{(0)} = \begin{pmatrix} -2 & 0 \\ 0 & 0 \end{pmatrix}, \quad n \in S, \quad \mathcal{H}_{n,n}^{(0)} = \begin{pmatrix} 1 & 0 \\ 0 & 1 \end{pmatrix}, \quad n \in \mathbb{Z} \setminus S. \quad (3.9)$$

Let $N = \dim(S) < \infty$. The spectrum of $\mathcal{H}^{(0)}\varphi = \gamma\varphi$ has exactly N negative eigenvalues $\gamma = -2$, N zero eigenvalues $\gamma = 0$ and infinitely many positive eigenvalues $\gamma = +1$. The negative and zero eigenvalues $\gamma = -2$ and $\gamma = 0$ map to N double zero eigenvalues $\lambda = 0$ in the eigenvalue problem $\mathcal{J}\mathcal{H}^{(0)}\psi = \lambda\psi$. The positive eigenvalues $\gamma = +1$ map to the infinitely many eigenvalues $\lambda = \pm i$.

Since finitely many zero eigenvalues of $\mathcal{J}\mathcal{H}^{(0)}$ are isolated from the rest of the spectrum, their shifts vanish as $\varepsilon \rightarrow 0$, according to the regular perturbation theory [38]. We can therefore locate small unstable eigenvalues $\operatorname{Re}(\lambda) > 0$ of the stability problem (3.7) for small $\varepsilon > 0$ from their limits at $\varepsilon = 0$. On the other hand, infinitely many imaginary eigenvalues of $\mathcal{J}\mathcal{H}^{(0)}$ become the continuous spectrum band as $\varepsilon \neq 0$ [39]. However, since the difference operator $\mathcal{J}\mathcal{H}$ has exponentially decaying potentials ϕ_n , $n \in \mathbb{Z}$, due to the decay condition (2.6), the continuous spectral bands of $\mathcal{J}\mathcal{H}$ are located on the imaginary axis of λ near the points $\lambda = \pm i$, similarly to the case for $\phi_n = 0$, $n \in \mathbb{Z}$ [39]. Therefore, the infinite-dimensional part of the spectrum does not produce any unstable eigenvalues $\operatorname{Re}(\lambda) > 0$ in the stability problem (3.7) as $\varepsilon > 0$. Results of the regular perturbation theory are formulated and proved below.

Lemma 3.1. *Assume that ϕ_n , $n \in \mathbb{Z}$, is the discrete soliton, described in Proposition 2.1. Let $N = \dim(S) < \infty$. Let γ_j , $1 \leq j \leq N$ be small eigenvalues of \mathcal{H} as $\varepsilon \rightarrow 0$ such that*

$$\lim_{\varepsilon \rightarrow 0} \gamma_j = 0, \quad 1 \leq j \leq N. \quad (3.10)$$

There exists $0 < \varepsilon_ \leq \varepsilon_0$ such that the eigenvalue problem (3.7) with ϕ_n , $n \in \mathbb{Z}$, and $0 < \varepsilon < \varepsilon_*$ has N pairs of small eigenvalues λ_j and $-\lambda_j$, $1 \leq j \leq N$, that satisfy the leading-order behavior*

$$\lim_{\varepsilon \rightarrow 0} \frac{\lambda_j^2}{\gamma_j} = 2, \quad 1 \leq j \leq N. \quad (3.11)$$

Proof. Since the operator \mathcal{L}_+ is Fredholm of zero index and empty kernel at $\varepsilon = 0$, it can be inverted for small $\varepsilon > 0$ and the non-self-adjoint eigenvalue problem (3.6) can be transformed to the self-adjoint diagonalization problem

$$\mathcal{L}_- \mathbf{w} = -\lambda^2 \mathcal{L}_+^{-1} \mathbf{w}, \quad (3.12)$$

such that

$$\lambda^2 = -\frac{(\mathbf{w}, \mathcal{L}_- \mathbf{w})_{\Omega}}{(\mathbf{w}, \mathcal{L}_+^{-1} \mathbf{w})_{\Omega}}, \quad (3.13)$$

where the inner product is defined in (3.3). Since all small eigenvalues of \mathcal{H} are small eigenvalues of \mathcal{L}_- , we denote by \mathbf{w}_j an eigenvector of \mathcal{L}_- which corresponds to the small eigenvalue γ_j , $1 \leq j \leq N$, in the limiting condition (3.10). By continuity of the eigenvectors and completeness of $\ker(\mathcal{L}_-^{(0)})$, there exists a set of normalized coefficients $\{c_{n,j}\}_{n \in S}$ for each $1 \leq j \leq N$ such that

$$\lim_{\varepsilon \rightarrow 0} \mathbf{w}_j = \mathbf{w}_j^{(0)} = \sum_{n \in S} c_{n,j} \mathbf{e}_n, \quad \sum_{n \in S} |c_{n,j}|^2 = 1, \tag{3.14}$$

where \mathbf{e}_n is the unit vector in Ω . It follows from the direct computations that

$$\lim_{\varepsilon \rightarrow 0} (\mathbf{w}_j, \mathcal{L}_+^{-1} \mathbf{w}_j) = (\mathbf{w}_j^{(0)}, \mathcal{L}_+^{(0)-1} \mathbf{w}_j^{(0)}) = -\frac{1}{2}. \tag{3.15}$$

The leading-order behavior (3.11) follows from (3.13) and (3.15) by the regular perturbation theory [38]. \square

Corollary 3.2. *Each small positive eigenvalue γ_j corresponds to a pair of positive and negative eigenvalues λ_j and $-\lambda_j$ for small $\varepsilon > 0$. Each small negative eigenvalue γ_j corresponds to a pair of purely imaginary eigenvalues λ_j and $-\lambda_j$ for small $\varepsilon > 0$. The latter eigenvalues have negative Krein signature:*

$$(\boldsymbol{\psi}, \mathcal{H}\boldsymbol{\psi}) = (\mathbf{u}, \mathcal{L}_+ \mathbf{u}) + (\mathbf{w}, \mathcal{L}_- \mathbf{w}) = 2(\mathbf{w}, \mathcal{L}_- \mathbf{w}) < 0. \tag{3.16}$$

For any $\varepsilon \neq 0$, there exists a simple zero eigenvalue of \mathcal{H} due to the gauge symmetry of the discrete solitons (2.2), as the parameter θ_0 is arbitrary, such that $\mathcal{L}_- \boldsymbol{\phi} = \mathbf{0}$. When all other $(N - 1)$ eigenvalues γ_j are non-zero for any $\varepsilon \neq 0$, the splitting of the semi-simple zero eigenvalue of $\mathcal{H}^{(0)}$ is called *generic*. The generic splitting gives a sufficient condition for unique (up to the gauge invariance) continuation of discrete solitons for $\varepsilon \neq 0$ [34], which is also guaranteed by Proposition 2.1 [24].

Let n_0 and p_0 be the numbers of negative and positive eigenvalues γ_j , defined in Lemma 3.1. The splitting is generic if $p_0 = N - 1 - n_0$. The numbers n_0 and p_0 are computed exactly from the limiting solution (2.5) as follows.

Lemma 3.3. *There exists $0 < \varepsilon_1 < \varepsilon_0$ such that the index n_0 for $0 < \varepsilon < \varepsilon_1$ equals the number of π -differences of the adjacent θ_n , $n \in S$, in the limiting solution (2.5), while $p_0 = N - 1 - n_0$.*

Proof. Since $\mathcal{L}_- \boldsymbol{\phi} = \mathbf{0}$ for any $0 < \varepsilon < \varepsilon_0$, the number n_0 of negative eigenvalues of \mathcal{L}_- coincides with the number of times when $\boldsymbol{\phi}$ changes sign, by the Discrete Sturm–Liouville Theorem [39]. In the case $\varepsilon = 0$, this number equals the number of π -differences of the adjacent θ_n , $n \in S$, in the limiting solution (2.5). By Lemma 2.3, the number remains continuous as $\varepsilon \neq 0$. The difference equation $\mathcal{L}_- \mathbf{w} = \mathbf{0}$ has only two fundamental solutions such that $\mathbf{w} = c_1 \mathbf{w}_1 + c_2 \mathbf{w}_2$, where c_1, c_2 are arbitrary parameters, $\mathbf{w}_1 = \boldsymbol{\phi}$ is exponentially decaying as $|n| \rightarrow \infty$, and \mathbf{w}_2 is exponentially growing as $|n| \rightarrow \infty$, due to the discrete Wronskian identity [39]. As a result, the kernel of \mathcal{L}_- is one-dimensional for $\varepsilon \neq 0$, such that $p_0 = N - 1 - n_0$. \square

It was recently studied [40,41] that there exists a closure relation between the negative index of the linearized Hamiltonian \mathcal{H} and the number of unstable eigenvalues of the linearized operator $\mathcal{J}\mathcal{H}$. The closure relation can be extended from the coupled NLS equations to the discrete NLS equations by using the same methods [40,41]. We hence formulate the closure relation for the discrete NLS equations (2.1).

Proposition 3.4. *Let $n(\mathcal{H})$ be the finite number of negative eigenvalues of \mathcal{H} . Let N_{real} be the number of positive real eigenvalues λ in the problem (3.7), N_{imag}^- be the number of pairs of purely imaginary eigenvalues λ with negative Krein signature $(\boldsymbol{\psi}, \mathcal{H}\boldsymbol{\psi}) < 0$, and N_{comp} be the number of complex eigenvalues λ in the first open quadrant of λ . Let $p(P') = 1$ if $P' \geq 0$ and $p(P') = 0$ if $P' < 0$, where*

$$P' = \|\boldsymbol{\phi}\|_{\Omega}^2 - \varepsilon \frac{d}{d\varepsilon} \|\boldsymbol{\phi}\|_{\Omega}^2. \tag{3.17}$$

Assume that $\lambda = 0$ is a double eigenvalue of the problem (3.7). Assume that no purely imaginary eigenvalues λ exist inside the continuous spectrum or have zero Krein signature. The indices above satisfy the closure relation

$$n(\mathcal{H}) - p(P') = N_{\text{real}} + 2N_{\text{imag}}^- + 2N_{\text{comp}}. \quad (3.18)$$

Proof. The left-hand side of (3.18) is the negative index of \mathcal{H} in the constrained subspace of Ω , which is reduced by one if the power $\|\phi\|_{\Omega}^2$ is a non-decreasing function of μ . Due to the scaling transformation (2.4), the derivative of $\|\phi\|_{\Omega}^2$ in μ is given by (3.17), where the hats for ϕ_n and ε are omitted. The right-hand side of (3.18) is the negative index of \mathcal{H} on the subspace of Ω , associated with the eigenvalue problem (3.6). The two indices are equal under the assumptions of the proposition, according to [40,41]. \square

Corollary 3.5. *There exists $0 < \varepsilon_2 < \varepsilon_1$ such that the indices of Proposition 3.4 for $0 < \varepsilon < \varepsilon_2$ are equal to the indices of Lemmas 3.1 and 3.3 as follows:*

$$n(\mathcal{H}) = N + n_0, \quad p(P') = 1, \quad N_{\text{real}} = N - 1 - n_0, \quad N_{\text{imag}}^- = n_0, \quad N_{\text{comp}} = 0, \quad (3.19)$$

and the closure relation (3.18) is met.

When the assumptions of Proposition 3.4 are not satisfied, instability bifurcations may occur in the eigenvalue problem (3.7), which results in the redistribution of the numbers $n(\mathcal{H})$, $p(P')$, N_{real} , N_{imag}^- , and N_{comp} . The Hamiltonian–Hopf bifurcation, which is typical for the discrete multi-humped solitons [29,31,33], occurs when the purely imaginary eigenvalues λ of negative Krein signature $(\psi, \mathcal{H}\psi) < 0$ collide with the purely imaginary eigenvalues λ of positive Krein signature $(\psi, \mathcal{H}\psi) > 0$ or with the continuous spectral band and bifurcate as complex unstable eigenvalues λ with $\text{Re}(\lambda) > 0$. It follows from Corollaries 3.2 and 3.5 that there can be at most n_0 Hamiltonian–Hopf instability bifurcations, which result in at most $N + n_0 - 1$ unstable eigenvalues, unless the indices $n(\mathcal{H})$ and $p(P')$ change as a result of the zero-eigenvalue bifurcations.

Combining Lemmas 3.1 and 3.3 and Corollaries 3.2 and 3.5, we summarize the main stability–instability result for the discrete solitons of the discrete NLS equation (2.1).

Theorem 3.6. *Let n_0 be the number of π -differences of the adjacent θ_n , $n \in S$, in the limiting solution (2.5). The discrete soliton is spectrally stable for small $\varepsilon > 0$ if and only if $n_0 = N - 1$. When $n_0 < N - 1$, the discrete soliton is spectrally unstable with exactly $N - 1 - n_0$ real unstable eigenvalues λ in the problem (3.7). When $n_0 \neq 0$, there exist n_0 pairs of purely imaginary eigenvalues λ with negative Krein signature, which may bifurcate to complex unstable eigenvalues λ away from the anti-continuum limit $\varepsilon \rightarrow 0$.*

The splitting of the zero eigenvalue of $\mathcal{H}^{(0)}$, which defines the stability–instability conclusion of Theorem 3.6, may occur in different powers of ε as $\varepsilon \rightarrow 0$. The power of ε , where it happens, depends on the set S , which classifies the family of the discrete solitons ϕ_n , $n \in \mathbb{Z}$. For the sets S_1 and S_2 , which are defined by (2.13) and (2.14), we show that the generic splitting of the zero eigenvalue occurs in the first and second orders of ε , respectively. These results are reported in the next two sections.

4. Bifurcations of the discrete solitons in the set S_1

Here we study the set S_1 with the explicit perturbation series expansions. These methods illustrate the general results of Theorem 3.6 and give asymptotic approximations for stable and unstable eigenvalues of the linearized stability problem (3.2). We compare the asymptotic and numerical approximations in the simplest cases $N = 2$ and $N = 3$.

By Lemma 2.2, the solution of the difference equations (2.8) is defined by the power series (2.9), where $\phi_n^{(0)}$ is given by (2.5) with $\theta_n = \{0, \pi\}$ for all $n \in S$ and $\phi_n^{(1)}$ solves the inhomogeneous problem

$$(1 - 3\phi_n^{(0)2})\phi_n^{(1)} = \phi_{n+1}^{(0)} + \phi_{n-1}^{(0)}, \quad n \in \mathbb{Z}. \quad (4.1)$$

For the set S_1 , defined by (2.13), the system (4.1) has the unique solution

$$\begin{aligned} \phi_n^{(1)} &= -\frac{1}{2}(\cos(\theta_{n-1} - \theta_n) + \cos(\theta_{n+1} - \theta_n))e^{i\theta_n}, & 2 \leq n \leq N - 1, \\ \phi_1^{(1)} &= -\frac{1}{2}\cos(\theta_2 - \theta_1)e^{i\theta_1}, & \phi_N^{(1)} &= -\frac{1}{2}\cos(\theta_N - \theta_{N-1})e^{i\theta_N}, \\ \phi_0^{(1)} &= e^{i\theta_1}, & \phi_{N+1}^{(1)} &= e^{i\theta_N}, \end{aligned} \tag{4.2}$$

while all other elements of $\phi_n^{(1)}$ are zero. The symmetric matrix \mathcal{H} is defined by the power series (3.8), where $\mathcal{H}^{(0)}$ is given by (3.9) and $\mathcal{H}^{(1)}$ consists of blocks:

$$\mathcal{H}_{n,n}^{(1)} = -2\phi_n^{(0)}\phi_n^{(1)} \begin{pmatrix} 3 & 0 \\ 0 & 1 \end{pmatrix}, \quad \mathcal{H}_{n,n+1}^{(1)} = \mathcal{H}_{n+1,n}^{(1)} = -\begin{pmatrix} 1 & 0 \\ 0 & 1 \end{pmatrix}. \tag{4.3}$$

while all other blocks of $\mathcal{H}_{n,m}^{(1)}$ are zero. The semi-simple zero eigenvalue of the problem $\mathcal{H}\varphi = \gamma\varphi$ is split as $\varepsilon > 0$ according to the perturbation series expansion

$$\varphi = \varphi^{(0)} + \varepsilon\varphi^{(1)} + O(\varepsilon^2), \quad \gamma = \varepsilon\gamma_1 + O(\varepsilon^2). \tag{4.4}$$

Let $\gamma = 0$ be a semi-simple eigenvalue of $\mathcal{H}^{(0)}$ with N linearly independent eigenvectors \mathbf{f}_n , $n \in S$. Recalling that $\sin \theta_n = 0$ and $\cos \theta_n = \pm 1$ for all $n \in S$, we normalize \mathbf{f}_n by the only non-zero block $(0, \cos \theta_n)^T$ at the n -th position, for convenience. The zero-order term $\varphi^{(0)}$ takes the form

$$\varphi^{(0)} = \sum_{n \in S} c_n \mathbf{f}_n, \tag{4.5}$$

where $c_n \in \mathbb{C}$, $n \in S$, are coefficients of the linear superposition. The first-order term $\varphi^{(1)}$ is found from the inhomogeneous system

$$\mathcal{H}^{(0)}\varphi^{(1)} = \gamma_1\varphi^{(0)} - \mathcal{H}^{(1)}\varphi^{(0)}. \tag{4.6}$$

Projecting the system (4.6) onto the kernel of $\mathcal{H}^{(0)}$, we find that the first-order correction γ_1 is defined by the reduced eigenvalue problem

$$\mathcal{M}_1\mathbf{c} = \gamma_1\mathbf{c}, \tag{4.7}$$

where $\mathbf{c} = (c_1, \dots, c_N)^T$ and \mathcal{M}_1 is a tri-diagonal N -by- N matrix, given by

$$(\mathcal{M}_1)_{m,n} = (\mathbf{f}_m, \mathcal{H}^{(1)}\mathbf{f}_n), \quad 1 \leq n, m \leq N, \tag{4.8}$$

or explicitly, based on the first-order solution (4.2) and (4.3):

$$\begin{aligned} (\mathcal{M}_1)_{n,n} &= \cos(\theta_{n+1} - \theta_n) + \cos(\theta_{n-1} - \theta_n), & 1 < n < N, \\ (\mathcal{M}_1)_{n,n+1} &= (\mathcal{M}_1)_{n+1,n} = -\cos(\theta_{n+1} - \theta_n), & 1 \leq n < N, \\ (\mathcal{M}_1)_{1,1} &= \cos(\theta_2 - \theta_1), & (\mathcal{M}_1)_{N,N} &= \cos(\theta_N - \theta_{N-1}). \end{aligned} \tag{4.9}$$

Similarly, the multiple zero eigenvalue of the problem $\mathcal{J}\mathcal{H}\psi = \lambda\psi$ is split as $\varepsilon > 0$ according to the perturbation series expansion

$$\psi = \psi^{(0)} + \sqrt{\varepsilon}\psi^{(1)} + \varepsilon\psi^{(2)} + O(\varepsilon\sqrt{\varepsilon}), \quad \lambda = \sqrt{\varepsilon}\lambda_1 + \varepsilon\lambda_2 + O(\varepsilon\sqrt{\varepsilon}). \tag{4.10}$$

Let $\lambda = 0$ be a multiple eigenvalue of $\mathcal{J}\mathcal{H}^{(0)}$ with N linearly independent eigenvectors \mathbf{f}_n , $n \in S$, and N linearly independent generalized eigenvectors \mathbf{g}_n , $n \in S$. The eigenvector \mathbf{g}_n has the only non-zero block $(\cos \theta_n, 0)^T$ at the

n -th position. The zero-order term is given by (4.5) as $\psi^{(0)} = \varphi^{(0)}$, while the first-order term $\psi^{(1)}$ is given by

$$\psi^{(1)} = \frac{\lambda_1}{2} \sum_{n \in S} c_n \mathbf{g}_n. \quad (4.11)$$

The second-order term $\psi^{(2)}$ is found from the inhomogeneous system

$$\mathcal{JH}^{(0)} \psi^{(2)} = \lambda_1 \psi^{(1)} + \lambda_2 \psi^{(0)} - \mathcal{JH}^{(1)} \psi^{(0)}. \quad (4.12)$$

Projecting the system (4.12) onto the kernel of $\mathcal{JH}^{(0)}$, we find that the first-order correction λ_1 is defined by the reduced eigenvalue problem

$$2\mathcal{M}_1 \mathbf{c} = \lambda_1^2 \mathbf{c}, \quad (4.13)$$

where \mathcal{M}_1 is given in (4.8). This result is in agreement with the leading-order behavior (3.11) of Lemma 3.1. The matrix \mathcal{M}_1 has the same structure as in the perturbation theory of continuous multi-pulse solitons [35]. Therefore, the number of positive and negative eigenvalues of \mathcal{M}_1 is defined by the following lemma.

Lemma 4.1. *Let n_0 , z_0 , and p_0 be the numbers of negative, zero, and positive terms of $a_n = \cos(\theta_{n+1} - \theta_n)$, $1 \leq n \leq N - 1$ such that $n_0 + z_0 + p_0 = N - 1$. The matrix \mathcal{M}_1 , defined by (4.9), has exactly n_0 negative eigenvalues, $z_0 + 1$ zero eigenvalues, and p_0 positive eigenvalues.*

Proof. See Lemma 5.4 and Appendix C of [35] for the proof. \square

When $z_0 = 0$, the zero eigenvalue of \mathcal{M}_1 with the eigenvector $(1, 1, \dots, 1)^T$ is unique. Since all $\theta_n = \{0, \pi\}$, $n \in S$, then all $a_n \neq 0$, $1 \leq j \leq N - 1$, such that $z_0 = 0$ and the splitting of the semi-simple zero eigenvalue of $\mathcal{H}^{(0)}$ is generic in the first order of ε for the set S_1 . By Lemma 4.1, stability and instability of the discrete solitons in the set S_1 are defined in terms of the number n_0 of π -differences in $\theta_{n+1} - \theta_n$ for $1 \leq n \leq N - 1$. This result is in agreement with Lemma 3.3 and Corollary 3.5 for the family S_1 . Thus, Theorem 3.6 for the set S_1 is verified with explicit perturbation series results.

We illustrate the stability results with two elementary examples of the discrete solitons in the set S_1 : $N = 2$ and $N = 3$. In the case $N = 2$, the discrete two-pulse solitons consist of the Page mode (a) and the twisted mode (b) as follows:

$$(a) \quad \theta_1 = \theta_2 = 0, \quad (b) \quad \theta_1 = 0, \quad \theta_2 = \pi. \quad (4.14)$$

The eigenvalues of matrix \mathcal{M}_1 are given explicitly as $\gamma_1 = 0$ and $\gamma_2 = 2 \cos(\theta_2 - \theta_1)$. Therefore, the Page mode (a) has one real unstable eigenvalue $\lambda \approx 2\sqrt{\varepsilon}$ in the stability problem (3.7) for small $\varepsilon > 0$, while the twisted mode (b) has no unstable eigenvalues but a simple pair of purely imaginary eigenvalues $\lambda \approx \pm 2i\sqrt{\varepsilon}$ with negative Krein signature. The latter pair may bifurcate to the complex plane as a result of the Hamiltonian–Hopf bifurcation.

These results are illustrated in Figs. 1 and 2, in agreement with numerical computations of the full problems (2.8) and (3.2). Fig. 1 shows the Page mode, while Fig. 2 corresponds to the twisted mode. The top subplots of each figure show the mode profiles (left) and the spectral plane $\lambda = \lambda_r + i\lambda_i$ of the linear eigenvalue problem (right) for $\varepsilon = 0.15$. The bottom subplots indicate the corresponding real (for the Page mode) and imaginary (for the twisted mode) eigenvalues from the theory (dashed line) versus the full numerical result (solid line). We find the agreement between the theory and the numerical computation to be excellent in the case of the Page mode (Fig. 1). For the twisted mode (Fig. 2), the agreement is within the 5% error for $\varepsilon < 0.0258$. For larger values of ε , the difference between the theory and numerics grows. The imaginary eigenvalues collide at $\varepsilon \approx 0.146$ with the band edge of the continuous spectrum such that the real part λ_r becomes non-zero for $\varepsilon > 0.146$.

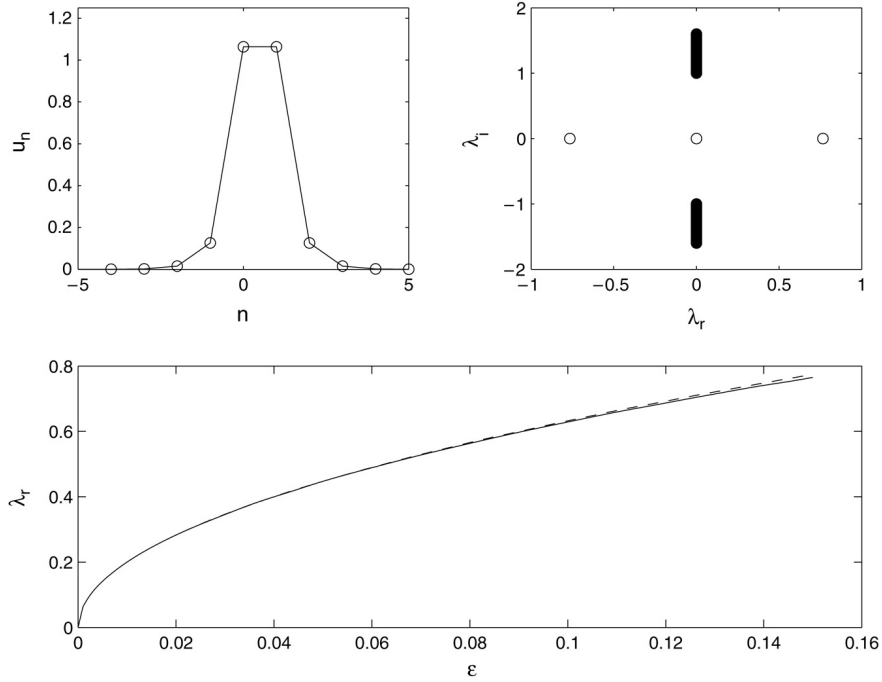


Fig. 1. The top panel shows the spatial profile of the Page mode (left) and the corresponding spectral plane of the linear stability problem (right) for $\varepsilon = 0.15$. The bottom subplot shows the continuation of the branch from $\varepsilon = 0$ to $\varepsilon = 0.15$ and the real positive eigenvalue theoretically (dashed line) and numerically (solid line).

In the case $N = 3$, the discrete three-pulse solitons consist of three modes as follows:

$$(a) \quad \theta_1 = \theta_2 = \theta_3 = 0, \quad (b) \quad \theta_1 = \theta_2 = 0, \quad \theta_3 = \pi, \quad (c) \quad \theta_1 = 0, \quad \theta_2 = \pi, \quad \theta_3 = 0. \quad (4.15)$$

The eigenvalues of matrix \mathcal{M}_1 are given explicitly as $\gamma_1 = 0$ and

$$\gamma_{2,3} = \cos(\theta_2 - \theta_1) + \cos(\theta_3 - \theta_2) \pm \sqrt{\cos^2(\theta_2 - \theta_1) - \cos(\theta_2 - \theta_1) \cos(\theta_3 - \theta_2) + \cos^2(\theta_3 - \theta_2)}.$$

The mode (a) has two real unstable eigenvalues $\lambda \approx \sqrt{6\varepsilon}$ and $\lambda \approx \sqrt{2\varepsilon}$ in the stability problem (3.7) for small $\varepsilon > 0$. The mode (b) has one real unstable eigenvalue $\lambda \approx \sqrt{2\sqrt{3}\varepsilon}$ and a simple pair of purely imaginary eigenvalues $\lambda \approx \pm i\sqrt{2\sqrt{3}\varepsilon}$ with negative Krein signature. This pair may bifurcate to the complex plane as a result of the Hamiltonian–Hopf bifurcation. The mode (c) has no unstable eigenvalues but two pairs of purely imaginary eigenvalues $\lambda \approx \pm i\sqrt{6\varepsilon}$ and $\lambda \approx \pm i\sqrt{2\varepsilon}$ with negative Krein signature. The two pairs may bifurcate to the complex plane as a result of the two successive Hamiltonian–Hopf bifurcations.

Figs. 3–5 summarize the results for the three modes (a)–(c), given in (4.15). Fig. 3 corresponds to the mode (a), where two real positive eigenvalues give rise to instability for any $\varepsilon \neq 0$. The error between theoretical and numerical results is within 5% for $\varepsilon < 0.15$ for one real eigenvalue and for $\varepsilon < 0.0865$ for the other eigenvalue. Similar results are observed on Fig. 4 for the mode (b), where the real positive eigenvalue and a pair of imaginary eigenvalues with negative Krein signature are generated for $\varepsilon > 0$. The imaginary eigenvalue collides with the band edge of the continuous spectrum at $\varepsilon \approx 0.169$, which results in the Hamiltonian–Hopf bifurcation. Finally, Fig. 5 shows the mode (c), where two pairs of imaginary eigenvalues with negative Krein signature exist for $\varepsilon > 0$. The first Hamiltonian–Hopf bifurcation occurs for $\varepsilon \approx 0.108$, while the second one occurs for much larger values of $\varepsilon \approx 0.223$, which is beyond the scale of Fig. 5.

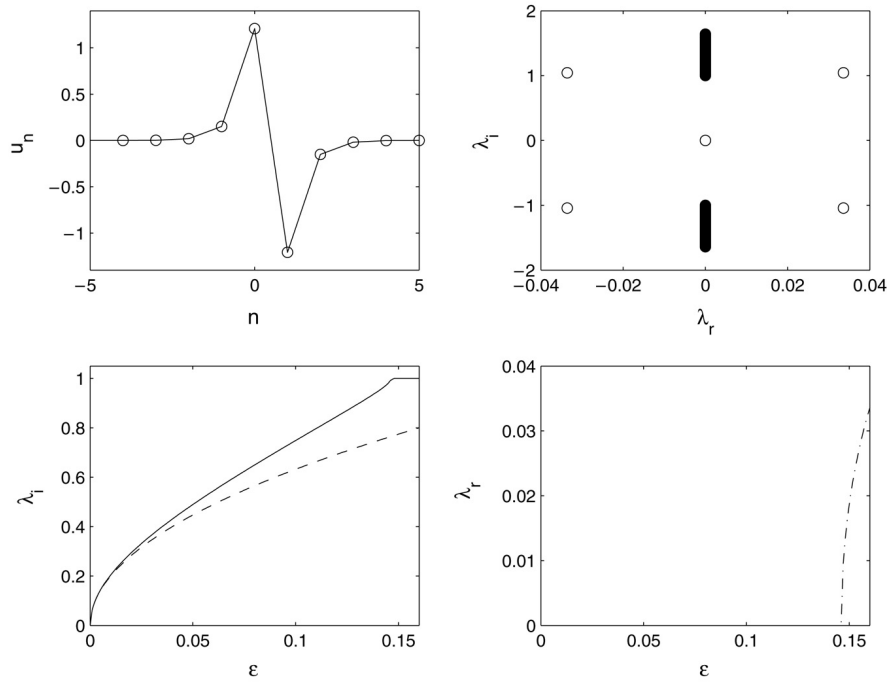


Fig. 2. The top panel shows the twisted mode and the spectral plane for $\varepsilon = 0.16$. The bottom subplot shows the imaginary and real parts of the eigenvalue with negative Krein signature, which bifurcates to the complex plane at $\varepsilon \approx 0.146$.

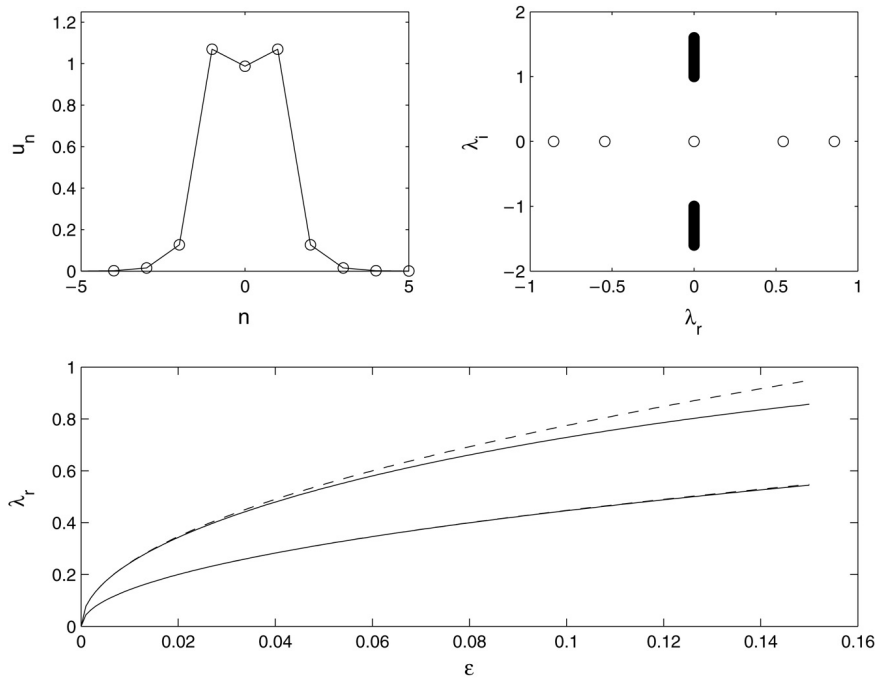


Fig. 3. Same as Fig. 1 but for the mode (a) with three excited sites in phase; $\varepsilon = 0.15$ in the top panels.

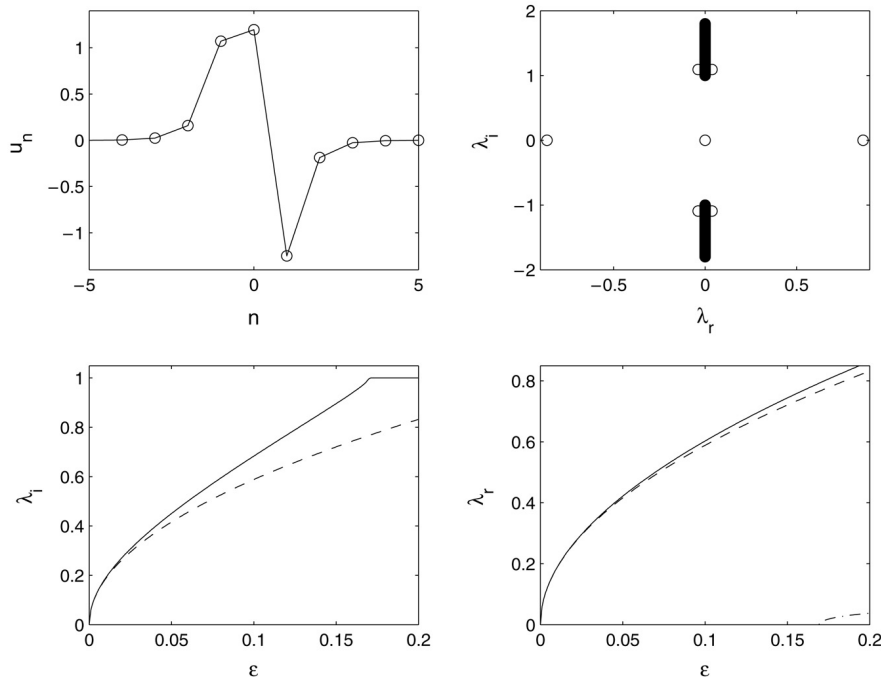


Fig. 4. Same as Fig. 2 but for the mode (b) with three excited sites, where the left and middle sites are in phase and the right π is out of phase; $\epsilon = 0.2$ in the top panels.

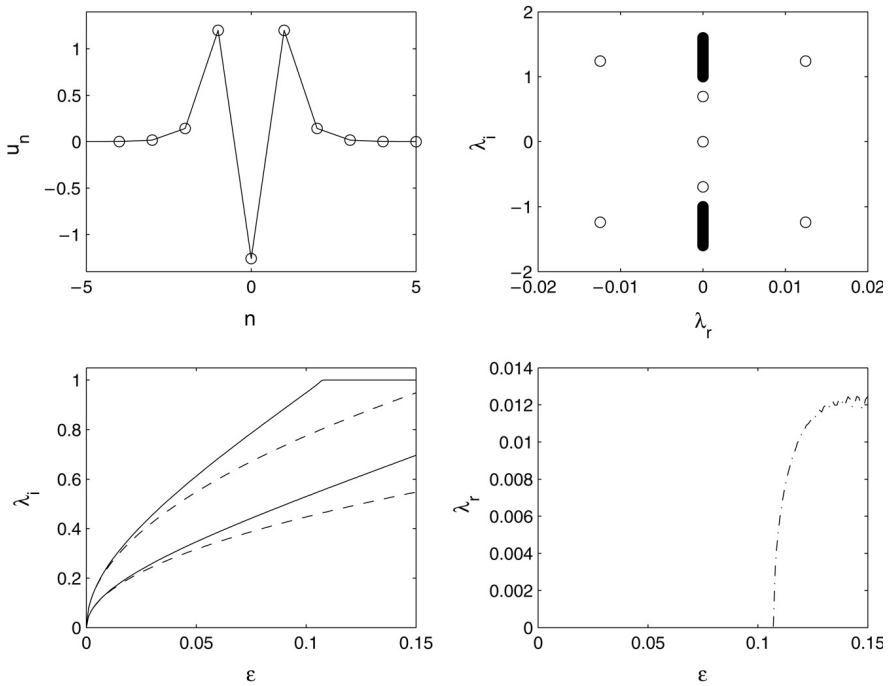


Fig. 5. Same as Fig. 2 but for the mode (c) with three excited sites, where adjacent sites are out of phase with each other.

5. Bifurcations of the discrete solitons in the set S_2

Here we study the set S_2 with the revised perturbation series expansions. The solution is defined by the power series (2.9), where the zero-order term $\phi_n^{(0)}$ is given by (2.5) with $\theta_n = \{0, \pi\}$ for all $n \in S$ and the first-order term $\phi_n^{(1)}$ is given by

$$\begin{aligned}\phi_n^{(1)} &= e^{i\theta_{n+1}} + e^{i\theta_{n-1}}, & n = 2m, \quad 1 \leq m \leq N-1, \\ \phi_0^{(1)} &= e^{i\theta_1}, & \phi_{2N}^{(1)} = e^{i\theta_{2N-1}},\end{aligned}\tag{5.1}$$

while all other elements of $\phi_n^{(1)}$ are zero. The second-order term $\phi_n^{(2)}$ solves the inhomogeneous problem

$$(1 - 3\phi_n^{(0)2})\phi_n^{(2)} = \phi_{n+1}^{(1)} + \phi_{n-1}^{(1)} + 3\phi_n^{(1)2}\phi_n^{(0)},\tag{5.2}$$

with the unique solution

$$\begin{aligned}\phi_n^{(2)} &= -\frac{1}{2}(\cos(\theta_{n+2} - \theta_n) + \cos(\theta_{n-2} - \theta_n) + 2)e^{i\theta_n}, & n = 2m-1, \quad 2 \leq m \leq N-1, \\ \phi_1^{(2)} &= -\frac{1}{2}(\cos(\theta_3 - \theta_1) + 2)e^{i\theta_1}, & \phi_{2N-1}^{(2)} = -\frac{1}{2}(\cos(\theta_{2N-1} - \theta_{2N-3}) + 2)e^{i\theta_{2N-1}}, \\ \phi_{-1}^{(2)} &= e^{i\theta_1}, & \phi_{2N+1}^{(2)} = e^{i\theta_{2N-1}},\end{aligned}\tag{5.3}$$

while all other elements of $\phi_n^{(2)}$ are zero. The symmetric matrix \mathcal{H} is defined by the power series (3.8), where the zero-order term $\mathcal{H}^{(0)}$ is given by (3.9) and the first-order term $\mathcal{H}^{(1)}$ is given by (4.3), where $\phi_n^{(0)}\phi_n^{(1)} = 0$, $n \in \mathbb{Z}$. The second-order term $\mathcal{H}^{(2)}$ has the structure

$$\mathcal{H}_{n,n}^{(2)} = -2\phi_n^{(0)}\phi_n^{(2)} \begin{pmatrix} 3 & 0 \\ 0 & 1 \end{pmatrix}, \quad n = 2m-1, \quad 1 \leq m \leq N\tag{5.4}$$

and

$$\mathcal{H}_{n,n}^{(2)} = -\phi_n^{(1)2} \begin{pmatrix} 3 & 0 \\ 0 & 1 \end{pmatrix}, \quad n = 2m, \quad 0 \leq m \leq N,\tag{5.5}$$

while all other blocks of $\mathcal{H}_{n,m}^{(2)}$ are zero. Similarly to in the previous section, the semi-simple zero eigenvalue of the problem $\mathcal{H}\varphi = \gamma\varphi$ is split as $\varepsilon > 0$ according to the modified perturbation series expansion

$$\varphi = \varphi^{(0)} + \varepsilon\varphi^{(1)} + \varepsilon\varphi^{(2)} + O(\varepsilon^3), \quad \gamma = \varepsilon^2\gamma_2 + O(\varepsilon^3),\tag{5.6}$$

where the zero-order term $\varphi^{(0)}$ is given by (4.5) and the first-order term $\varphi^{(1)}$ has the form

$$\varphi^{(1)} = \sum_{n \in S} c_n (\mathcal{S}_+ \mathbf{f}_n + \mathcal{S}_- \mathbf{f}_n),\tag{5.7}$$

where \mathcal{S}_\pm are shift operators of the non-zero 2-block of \mathbf{f}_n up and down. The second-order term $\varphi^{(2)}$ is found from the inhomogeneous system

$$\mathcal{H}^{(0)}\varphi^{(2)} = \gamma_2\varphi^{(0)} - \mathcal{H}^{(1)}\varphi^{(1)} - \mathcal{H}^{(2)}\varphi^{(0)}.\tag{5.8}$$

Projecting the system (5.8) onto the kernel of $\mathcal{H}^{(0)}$, we find the reduced eigenvalue problem

$$\mathcal{M}_2 \mathbf{c} = \gamma_2 \mathbf{c},\tag{5.9}$$

where $\mathbf{c} = (c_1, c_3, \dots, c_{2N-1})^T$ and \mathcal{M}_2 is the tri-diagonal N -by- N matrix, given by

$$(\mathcal{M}_2)_{m,n} = (\mathbf{f}_{2m-1}, \mathcal{H}^{(2)}\mathbf{f}_{2n-1}) + (\mathbf{f}_{2m-1}, \mathcal{H}^{(1)}(\mathcal{S}_+ + \mathcal{S}_-)\mathbf{f}_{2n-1}),\tag{5.10}$$

for $1 \leq n, m \leq N$, or explicitly, based on the first-order and second-order solutions (5.1) and (5.3):

$$\begin{aligned} (M_2)_{n,n} &= \cos(\theta_{2n+1} - \theta_{2n-1}) + \cos(\theta_{2n-3} - \theta_{2n-1}), & 1 < n < N, \\ (M_2)_{n,n+1} &= (M_2)_{n+1,n} = -\cos(\theta_{2n+1} - \theta_{2n-1}), & 1 \leq n < N, \\ (M_2)_{1,1} &= \cos(\theta_3 - \theta_1), & (M_2)_{N,N} = \cos(\theta_{2N-1} - \theta_{2N-3}). \end{aligned} \quad (5.11)$$

Similarly, the multiple zero eigenvalue of the problem $\mathcal{JH}\psi = \lambda\psi$ is split as $\varepsilon > 0$ according to the modified perturbation series expansion

$$\psi = \psi^{(0)} + \varepsilon\psi^{(1)} + \varepsilon^2\psi^{(2)} + O(\varepsilon^3), \quad \lambda = \varepsilon\lambda_1 + \varepsilon^2\lambda_2 + O(\varepsilon^3), \quad (5.12)$$

where the zero-order term $\psi^{(0)} = \varphi^{(0)}$ is given by (4.5) and the first-order term $\psi^{(1)}$ has the form

$$\psi^{(1)} = \sum_{n \in S} c_n (\mathcal{S}_+ \mathbf{f}_n + \mathcal{S}_- \mathbf{f}_n) + \frac{\lambda_1}{2} \sum_{n \in S} c_n \mathbf{g}_n. \quad (5.13)$$

The second-order term $\psi^{(2)}$ is found from the inhomogeneous system

$$\mathcal{JH}^{(0)}\psi^{(2)} = \lambda_1\psi^{(1)} + \lambda_2\psi^{(0)} - \mathcal{JH}^{(1)}\psi^{(1)} - \mathcal{JH}^{(2)}\psi^{(0)}. \quad (5.14)$$

Projecting the system (5.14) onto the kernel of $\mathcal{JH}^{(0)}$, we find the reduced eigenvalue problem

$$2\mathcal{M}_2\mathbf{c} = \lambda_1^2\mathbf{c}, \quad (5.15)$$

in accordance with Lemma 3.1. Since the matrix \mathcal{M}_2 has exactly the structure of the matrix \mathcal{M}_1 , described in Lemma 4.1, we conclude that the stability and instability of the discrete solitons in the set S_2 are defined in terms of the number n_0 of π -differences in $\theta_{2n+1} - \theta_{2n-1}$, $1 \leq n \leq N - 1$, in accordance with Lemma 3.3 and Corollary 3.5. Thus, Theorem 3.6 for the set S_2 is verified with explicit perturbation series results.

We summarize that the bifurcations and stability of the discrete solitons in the set S_2 are exactly equivalent to those in the set S_1 , but the splitting of all zero eigenvalues occurs in the order of ε^2 , rather than in the order of ε . These results for the set S_2 with $N = 2$ and $N = 3$ are shown on Figs. 6–10, in full analogy with those for the set S_1 . The corresponding asymptotic approximations of eigenvalues can be “translated” from those of the previous section by substituting $\sqrt{\varepsilon} \rightarrow \varepsilon$. Fig. 6 shows the Page mode where the agreement with the theory is excellent for $\varepsilon < 0.2$. Fig. 7 shows the twisted mode with very good agreement for $\varepsilon < 0.415$ and the Hamiltonian–Hopf bifurcation at $\varepsilon \approx 0.431$. The only difference from the twisted mode of Fig. 2 is that the imaginary eigenvalue of negative Krein signature collides with the imaginary eigenvalue of positive Krein signature, rather than with the band edge of the continuous spectrum. Figs. 8–10 show the modes (a), (b), and (c), respectively, of the three excited sites. Again, the Hamiltonian–Hopf bifurcations occur when the imaginary eigenvalues of negative Krein signature collide with the imaginary eigenvalues of positive Krein signature. For the mode (b), the bifurcation occurs at $\varepsilon \approx 0.328$ (see Fig. 9). For the mode (c), two bifurcations occur at $\varepsilon \approx 0.375$ and $\varepsilon \approx 0.548$ (see Fig. 10).

6. Summary

We have studied the stability of discrete solitons in the one-dimensional NLS lattice (1.1) with $d = 1$. We have rigorously proved the numerical conjecture that the discrete solitons with anti-phase excited nodes are stable near the anti-continuum limit, while all other discrete solitons are linearly unstable with real positive eigenvalues in the stability problem. Additionally, we gave a precise count of the real eigenvalues and pairs of imaginary eigenvalues with negative Krein signature. These results are not affected if the excited nodes are separated by an arbitrary sequence of empty nodes. We studied two particular sets of discrete solitons with explicit perturbation series expansions and numerical approximations and found very good agreement between the asymptotic and numerical computations.

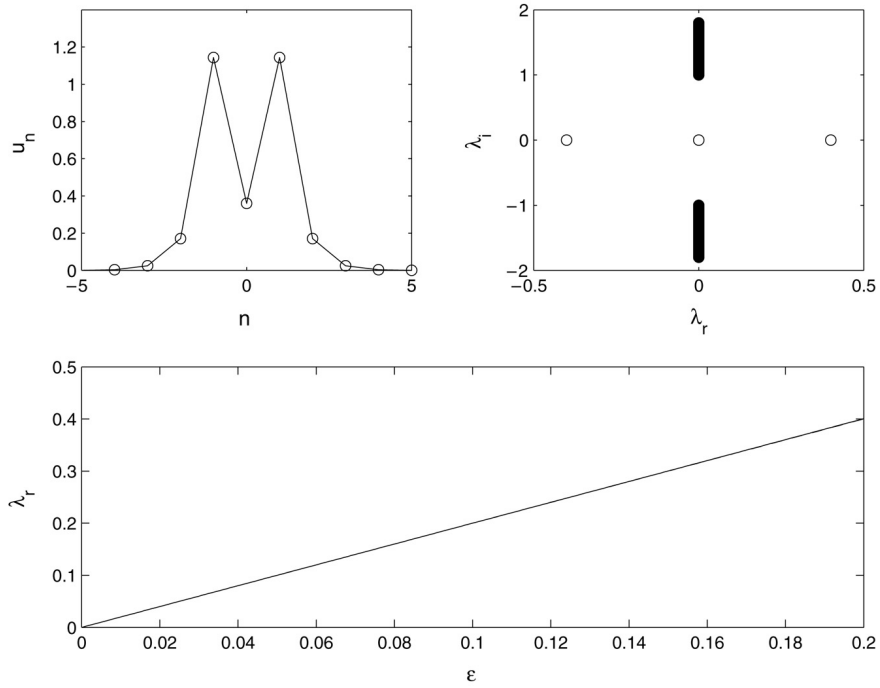


Fig. 6. Same as Fig. 1 but for the Page mode of the set S_2 ; $\epsilon = 0.2$ in the top panels.

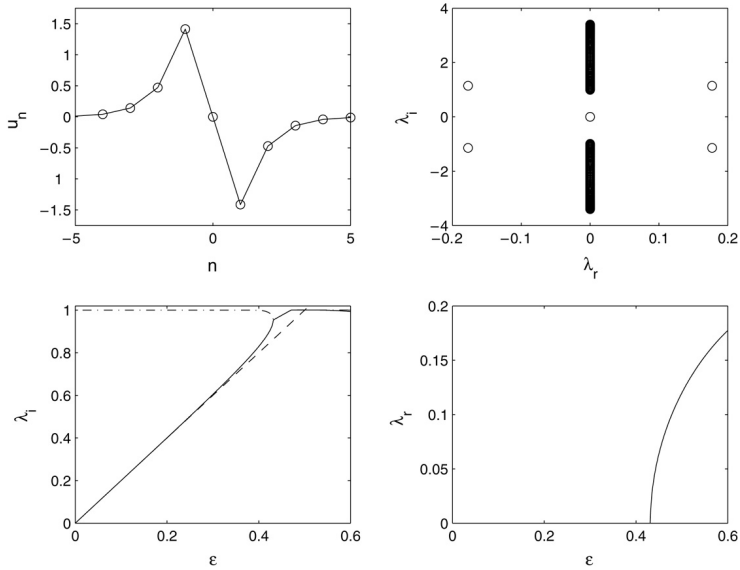


Fig. 7. Same as Fig. 2 but for the twisted mode of the set S_2 ; $\epsilon = 0.6$ in the top panels.

The stability and instability results remain invariant if the discrete solitons are excited in the two-dimensional NLS lattice (1.1) with $d = 2$ such that the set S is an open discrete contour on the plane. Similar perturbation series

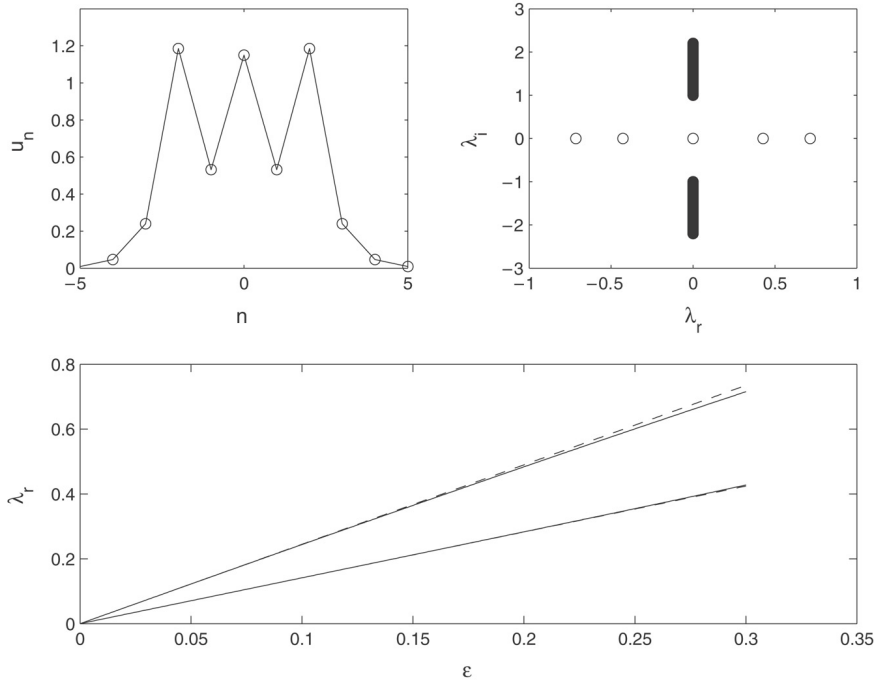


Fig. 8. Same as Fig. 3 but for the mode (a) of the set S_2 ; $\epsilon = 0.3$ in the top panels.

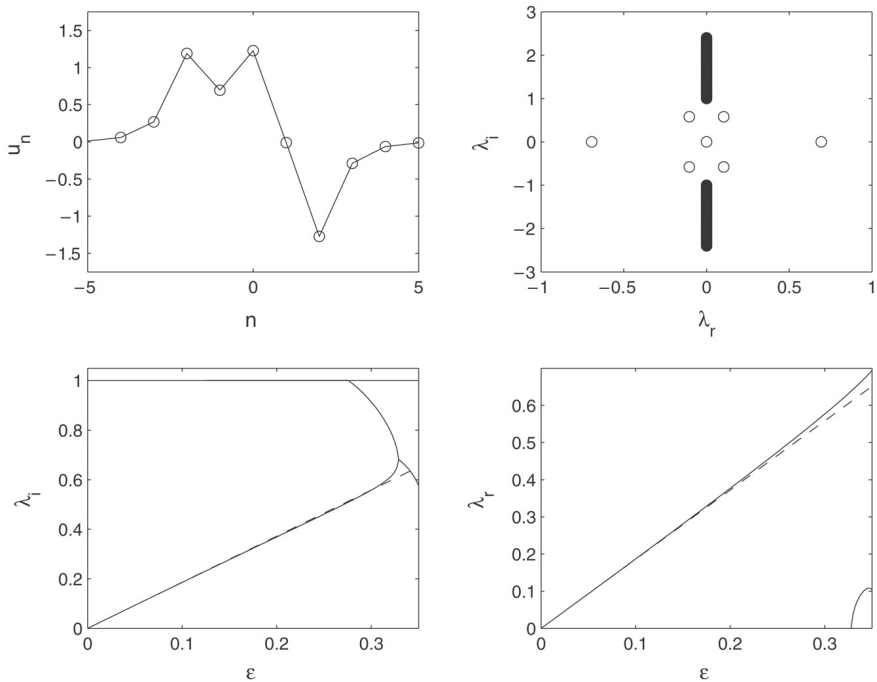


Fig. 9. Same as Fig. 4 but for the mode (b) of the set S_2 ; $\epsilon = 0.35$ in the top panels.

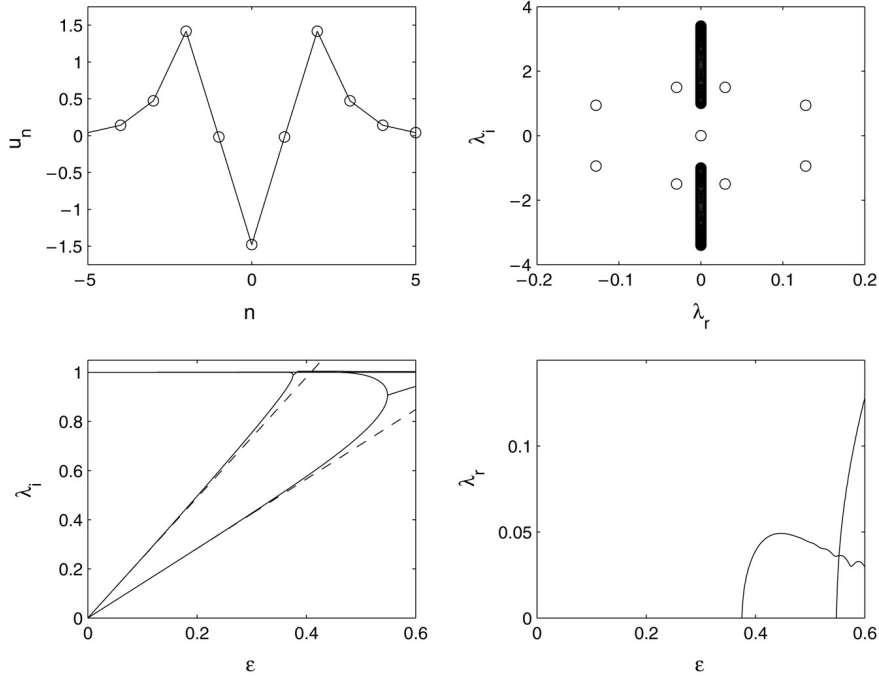


Fig. 10. Same as Fig. 5 but for the mode (c) of the set S_2 ; $\varepsilon = 0.6$ in the top panels.

expansions for the sets S_1 and S_2 in the two-dimensional NLS lattice can be developed and the same matrices \mathcal{M}_1 and \mathcal{M}_2 define the stability and instability of these discrete solitons.

In a separate paper, we shall consider a closed discrete contour on the plane for the set S . Such sets may support both discrete solitons and discrete vortices with a non-zero topological charge. Continuation of the limiting solutions from $\varepsilon = 0$ to $\varepsilon \neq 0$ is a non-trivial problem if the amplitudes ϕ_n are complex-valued. It would then be relevant to study the persistence, multiplicity and stability of such continuations with the methods of Lyapunov–Schmidt reductions.

Acknowledgements

This work was partially supported by NSF-DMS-0204585, NSF-CAREER, and the Eppley Foundation for Research (PGK) and by NSERC grant (DEP). PGK is also particularly grateful to G.L. Alfimov, V.A. Brazhnyi, and V.V. Konotop for numerous insightful discussions regarding discrete soliton stability and for their communication of details of their work [19] prior to publication.

References

- [1] H.S. Eisenberg, R. Morandotti, Y. Silberberg, J.M. Arnold, G. Pennelli, J.S. Aitchison, Optical discrete solitons in waveguide arrays. I. Soliton formation, *J. Opt. Soc. Amer. B* 19 (2002) 2938–2944.
- [2] U. Peschel, R. Morandotti, J.M. Arnold, J.S. Aitchison, H.S. Eisenberg, Y. Silberberg, T. Pertsch, F. Lederer, Optical discrete solitons in waveguide arrays. 2. Dynamic properties, *J. Opt. Soc. Amer. B* 19 (2002) 2637–2644.
- [3] N.K. Efremidis, S. Sears, D.N. Christodoulides, J.W. Fleischer, M. Segev, Discrete solitons in photorefractive optically induced photonic lattices, *Phys. Rev. E* 66 (2002) 046602.

- [4] A.A. Sukhorukov, Yu.S. Kivshar, H.S. Eisenberg, Y. Silberberg, Spatial optical solitons in waveguide arrays, *IEEE J. Quantum Electron.* 39 (2003) 31–50.
- [5] F.S. Cataliotti, S. Burger, C. Fort, P. Maddaloni, F. Minardi, A. Trombettoni, A. Smerzi, M. Inguscio, Josephson junction arrays with Bose–Einstein condensates, *Science* 293 (2001) 843–846.
- [6] F.S. Cataliotti, L. Fallani, F. Ferlaino, C. Fort, P. Maddaloni, M. Inguscio, Superfluid current disruption in a chain of weakly coupled Bose–Einstein condensates, *New J. Phys.* 5 (2003) 71.
- [7] F.Kh. Abdullaev, B.B. Baizakov, S.A. Darmanyan, V.V. Konotop, M. Salerno, Nonlinear excitations in arrays of Bose–Einstein condensates, *Phys. Rev. A* 64 (2001) 043606.
- [8] G.L. Alfimov, P.G. Kevrekidis, V.V. Konotop, M. Salerno, Wannier functions analysis of the nonlinear Schrödinger equation with a periodic potential, *Phys. Rev. E* 66 (2002) 046608.
- [9] M.V. Fistul, Resonant breather states in Josephson coupled systems, *Chaos* 13 (2003) 725–732.
- [10] J.J. Mazo, T.P. Orlando, Discrete breathers in Josephson arrays, *Chaos* 13 (2003) 733–743.
- [11] T. Dauxois, M. Peyrard, A.R. Bishop, Entropy-driven DNA denaturation, *Phys. Rev. E* 47 (1993) R44–R47.
- [12] M. Peyrard, T. Dauxois, H. Hoyet, C.R. Willis, Biomolecular dynamics of DNA—Statistical-mechanics and dynamical models, *Phys. D* 68 (1993) 104–115.
- [13] S. Aubry, Breathers in nonlinear lattices: existence, linear stability and quantization, *Phys. D* 103 (1997) 201–250.
- [14] S. Flach, C.R. Willis, Discrete breathers, *Phys. Rep.* 295 (1998) 181–264.
- [15] D. Hennig, G. Tsironis, Wave transmission in nonlinear lattices, *Phys. Rep.* 307 (1999) 333–432.
- [16] P.G. Kevrekidis, K.O. Rasmussen, A.R. Bishop, The discrete nonlinear Schrödinger equation: A survey of recent results, *Int. J. Mod. Phys. B* 15 (2001) 2833–2900.
- [17] J.Ch. Eilbeck, M. Johansson, in: L. Vazquez, R.S. MacKay, M.P. Zorzano (Eds.), *Localization and Energy Transfer in Nonlinear Systems*, World Scientific, Singapore, 2003, p. 44.
- [18] M. Peyrard, Yu.S. Kivshar, Modulational instabilities in discrete lattices, *Phys. Rev. A* 46 (1992) 3198–3205.
- [19] G.L. Alfimov, V.A. Brazhnyi, V.V. Konotop, On classification of intrinsic localized modes for the discrete nonlinear Schrödinger equation, *Phys. D* 194 (2004) 127–150.
- [20] H.R. Dullin, J.D. Meiss, Generalized Henon maps: the cubic diffeomorphisms of the plane, *Phys. D* 143 (2000) 262–289.
- [21] J.M. Bergamin, T. Bountis, C. Jung, A method for locating symmetric homoclinic orbits using symbolic dynamics, *J. Phys. A: Math. Gen.* 33 (2000) 8059–8070.
- [22] J.M. Bergamin, T. Bountis, M.N. Vrahatis, Homoclinic orbits of invertible maps, *Nonlinearity* 15 (2002) 1603–1619.
- [23] S. Aubry, G. Abramovici, Chaotic trajectories in the standard map—the concept of antiintegrability, *Phys. D* 43 (1990) 199–219.
- [24] R.S. MacKay, S. Aubry, Proof of existence of breathers for time-reversible or Hamiltonian networks of weakly coupled oscillators, *Nonlinearity* 7 (1994) 1623–1643.
- [25] L. Nirenberg, *Topics in Nonlinear Functional Analysis*, Courant Institute, NY, 1974.
- [26] M. Weinstein, Excitation thresholds for nonlinear localized modes on lattices, *Nonlinearity* 12 (1999) 673–691.
- [27] T. Kapitula, P.G. Kevrekidis, Stability of waves in discrete systems, *Nonlinearity* 14 (2001) 533–566.
- [28] M. Johansson, S. Aubry, Existence and stability of quasiperiodic breathers in the discrete nonlinear Schrödinger equation, *Nonlinearity* 10 (1997) 1151–1178.
- [29] P.G. Kevrekidis, A.R. Bishop, K.O. Rasmussen, Twisted localized modes, *Phys. Rev. E* 63 (2001) 036603.
- [30] T. Kapitula, P.G. Kevrekidis, B.A. Malomed, Stability of multiple pulses in discrete systems, *Phys. Rev. E* 63 (2001) 036604.
- [31] P.G. Kevrekidis, M.I. Weinstein, Breathers on a background: periodic and quasiperiodic solutions of extended discrete nonlinear wave systems, *Math. Comput. Simulation* 62 (2003) 65–78.
- [32] A.M. Morgante, M. Johansson, G. Kopidakis, S. Aubry, Standing wave instabilities in a chain of nonlinear coupled oscillators, *Phys. D* 162 (2002) 53–94.
- [33] M. Johansson, Hamiltonian Hopf bifurcations in the discrete nonlinear Schrödinger equation, *J. Phys. A: Math. Gen.* 37 (2004) 2201–2222.
- [34] B. Sandstede, C.K.R.T. Jones, J.C. Alexander, Existence and stability of N -pulses on optical fibers with phase-sensitive amplifiers, *Phys. D* 106 (1997) 167–206.
- [35] B. Sandstede, Stability of multiple-pulse solutions, *Trans. Amer. Math. Soc.* 350 (1998) 429–472.
- [36] T. Kapitula, Stability of waves in perturbed Hamiltonian systems, *Phys. D* 156 (2001) 186–200.
- [37] T. Kapitula, P.G. Kevrekidis, Linear stability of perturbed Hamiltonian systems: theory and a case example, *J. Phys. A: Math. Gen.* 37 (2004) 7509–7526.
- [38] R. Horn, C. Johnson, *Matrix Analysis*, Cambridge University Press, 1985.
- [39] H. Levy, F. Lessman, *Finite Difference Equations*, Dover, New York, 1992.
- [40] D. Pelinovsky, Inertia law for spectral stability of solitary waves in coupled nonlinear Schrödinger equations, *Proc. Roy. Soc. Lond. A* 461 (2005) 783–812. Preprint available at <http://dmpeli.math.mcmaster.ca/PaperBank/diagonalization.pdf>.
- [41] T. Kapitula, P.G. Kevrekidis, B. Sandstede, Counting eigenvalues via the Krein signature in infinite-dimensional Hamiltonian systems, *Phys. D* 195 (2004) 263–282.